Polarization of an exciton in a ZnO layer using a split gate potential

P. A. Sundqvist,* Q. X. Zhao, and M. Willander
Physical Electronics and Photonics, Department of Physics, Fysikgränd 3, University of Göteborg and Chalmers University of Technology, S-412 96 Göteborg, Sweden

(Received 27 February 2003; revised manuscript received 9 June 2003; published 31 October 2003)

In this paper we focus on structural and optical transitions of an exciton in a Zinc Oxide (ZnO) layer, which could be widely controlled by a split gate potential. We have solved the exciton problem by a self-consistent Schrödinger-Poisson technique, where the Hamiltonian includes the boundary conditions for the split gate structure. The gate voltage creates a paraboliclike potential, which at a typical threshold voltage separates or polarizes the exciton strongly. This sharp structural transition brings the exciton from being strongly correlated with a large overlap to a regime where the correlation is very small (with small overlap). The resulting structure for the exciton at negative gate voltages is a structure where the hole is located like a ring around a dotlike electron. For positive values of the gate voltage the situation is opposite. We have especially studied the ground-state binding energy and the optical transitions of the exciton. We found that the ground-state energy for ZnO could be tuned and the decrease of the ground-state energy can be as large as the double of the bulk exciton energy (60 meV for ZnO) with a gate voltage of -5 V. The ground-state energy is almost constant for small values of the gate voltage but at a typical threshold voltage (approximately -2 V) the energy suddenly changes and becomes linear with the gate voltage. We also analyze the lifetime for the exciton, which is shown to increase from nanoseconds to beyond milliseconds. This was shown to be an effect of the small overlap between the hole and the electron when the gate voltage increased above the threshold voltage. Stimulated by the long lifetime of the ground state of the exciton we also calculated the optical transition frequency and the corresponding oscillator strength for the transition between the ground state and the dominating excited (self-consistent) exciton states. The transition frequency was found to occur in the THz region and the oscillator strength in the range of 0.3–0.4 for gate voltages between -2 V and -5 V. In addition, we have also analytically described polarization and especially total charge densities for excitons in small linear electric fields.

DOI: 10.1103/PhysRevB.68.155334 PACS number(s): 71.35.Lk, 73.20.Mf, 71.35.Cc

I. INTRODUCTION

Excitons are rare objects in nature due to their short lifetime but are ideal study objects from a theoretical point of view since their ground-state energy can be measured experimentally. This opportunity is possible since they are created from the vacuum state by laser light. Experimentally the absorption peak of an exciton appears at $E_G - E_0$,[1] where E_G is the band gap of the material (corresponding to breaking a covalent bond) and E_0 is the binding energy of the ground state (due to Coulomb attraction). Since the band gap is known, one could experimentally verify a theoretical quantum calculation for the ground state. This is normally not the case for other types of quantum problems (such as few electron systems in a quantum dot), where only transition energies between different states could be experimentally detected. A verification of these kinds of calculations must then be performed indirectly by a measurement of the charge density, normally using a tunneling tip.[2]

The excitons confined in low-dimensional semiconductor heterostructures are particularly interesting, due to enhancement of the exciton binding energy. The fast progress of the epitaxy growth such as molecular-beam epitaxy (MBE) have made it possible to grow high quality quantum well, quantum wire, and quantum dot structures. The excitons confined in two-dimensional (2D) heterostructures have been investigated extensively during the last three decades.[3,4] The calculated exciton binding energies (for calculations see, for example, Refs. 5–7) in various structures have been compared with experimental observations (for experiments see, for example, Ref. 8) and they show a good agreement (compare, for instance, Refs. 9,10), resulting in a comprehensive understanding of the excitons in those low-dimensional structures. However, due to the small value of the exciton binding energy, the experimental investigations have to be conducted at low temperatures. In addition, there are very limited investigations on the intralevel transitions of the excitons.[11] Because the exciton lifetime is short and the transition energy is extremely small, such intralevel transitions have no practical applications and are difficult to investigate experimentally.

There have been several approaches to solve exciton problems, such as variational approaches,[12] dynamical Coulomb screening approaches,[13] Hartree and Ritz approaches,[15] and ladder diagram approaches.[16]

Special optical effects of excitons such as in Bose-Einstein condensation have been reported for exciton systems[17] as well as structural transition phenomena in excitons when a magnetic field is applied.[18] Also, the existence of surface excitons have been analyzed.[19] A good review of excitons in heterostructures could be found in a book by Ivchenko and Pikus.[20]

In this study we choose the Zinc Oxide (ZnO) system. One of the first calculations that was performed on ZnO was made by Büttner and Pollman,[13] who also treated the exciton-phonon interaction. ZnO is a direct band gap wurtzite-type semiconductor with a band gap energy of 3.37

eV at room temperature. Furthermore, due to the extremely large exciton binding energy (about 60 meV), the excitons in ZnO are thermally stable at room temperature. Thus, ZnO has significant advantage in optoelectronic applications such as the ultraviolet lasing media. In addition, due to the large exciton binding energy, the specific device (the spilt gate setup) can be used to tune the exciton lifetime, and this as well as the stable exciton at room temperature making use of the exciton intralevel transitions becomes possible.

ZnO is a strong polar material with strong polaron effects. In this paper we ignore the exciton-phonon interaction (besides the creation and destruction of the exciton in interaction with the photon field). These effects are expected to significantly modify the exciton energy,[13] especially in low-dimensional structures. These effects are known to screen the Coulomb interaction between the electron and the hole. We use however a simple model with a pure static Coulomb interaction in which the rather complex polarization response of the crystal due to the electric fields generated by the electron and the hole is baked together into the dielectric constant ε. Also the fact that the exciton has a very short lifetime results in that the crystal would respond (i.e., polarize) to the excitonic electric fields for a very short time. Therefore, the choice of the static value of ε is not totally satisfactory. We believe however that our model, with a value of ε fitted to give the correct experimental value of the ground-state energy (for the bulk exciton), serves well to explain the trends described in this paper. To the authors' knowledge this perhaps unconventional method has never been used before. On the contrary, the use of the static value of ε would give a much more inaccurate result in comparison with the experimental values.

In this paper we demonstrate theoretically how split gates could be used to strongly polarize an exciton and show also how realistic calculations could be performed using boundary-condition dependent Hamiltonians, resulting in coupled Schrödinger-Poisson equations. In addition, we considered the question of the lifetime of the exciton. A similar Hartree calculation has been done by Janssens *et al.* on a two-dimensional type II quantum dot, using a magnetic field.[14] In their paper they show that a variation of the potential barriers gives rise to a transition of the exciton structure. This effect is almost the same as we present here, but in our case we obtain the same effect by altering a split gate voltage, which at a certain threshold voltage breaks up the bulklike exciton structure to a strongly polarized exciton, where the hole is located as a ring around a dotlike electron. The benefit with our model is of course that the voltage is easy to change, meanwhile a potential barrier must be varied by altering the material in the type II quantum dot. On the other hand, the metal gate in our case would give rise to image charges (which are more difficult to treat) and this problem does appear in a type II quantum dot.

In Sec. II we describe the split gate setup that defines nonlinear potentials that could be created from it. In Sec. III we give the theory for the exciton lifetime, polarization, and charge density for perturbational hydrogenlike excitons, the theory for boundary-condition dependent Hamiltonians in the Hartree model for the excitons and finally the optical transition rules for optical excitations between intralevels of the excitons. The split gate structure details such as geometry, dimensions, and boundary conditions as well as the numerical results are given in Sec. IV. Section V is devoted to conclusions.

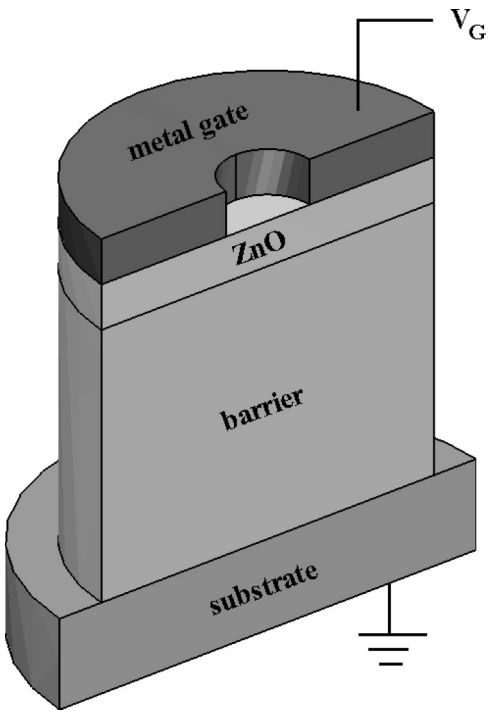

FIG. 1. A metal split gate on the top of a ZnO layer (not to scale). A voltage V_G is applied between the metal gate and the grounded substrate.

II. THE SPLIT GATE SETUP

The principal setup of the split gate is shown in Fig. 1. It is not necessary to etch out the outer cylindrical part of the structure for the device operation (It is shown in this way for clarity). The barrier material and the ZnO layer could be grown on the substrate using, for example, molecular-beam epitaxy (MBE). The fabrication of the hole in the metal gate could easily be done by E-beam lithography and lift-off technique. Today's contemporary E-beam machines can make such spots with a diameter down to 15–20 nm. The barrier material could be a related material to ZnO, for example, ZnMgO. It is assumed that the substrate is heavily doped or is a metal layer so that the potential would be constant here.

We use a cylindrical coordinate system to describe the structure of the split gate. The coordinate z is zero at the interface between the ZnO and the metal gate, and goes vertically upwards in the figure. The ZnO is then placed at $-L<z<0$, where L is the thickness of the ZnO layer. The radial coordinate ρ goes outward from the center of the hole in the metal gate. The diameter of the hole is 18.9 nm, which corresponds to 10 bohrs radii of the ZnO exciton (bulk). The distance from the metal gate down to the grounded substrate is 151 nm (corresponding to 291 atomic layers of ZnO). The thickness of the ZnO layer L varies in our calculation.

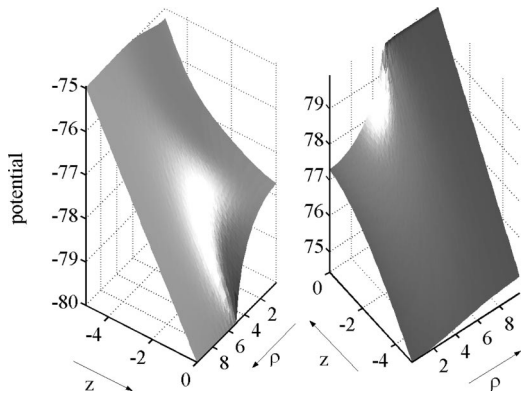

FIG. 2. Split gate potential felt by a hole (to the left) and an electron (to the right). Note that the axes are rotated to show the potential from the ''best'' view. The hole will be driven outwards in the radial direction and up to the metal gate ($z=0$). The electron will be driven towards $\rho=0$ and will ''roll down'' to the substrate, but will be stopped by a barrier (not shown in this picture).

The potential for an electron or a hole could be estimated by solving the Laplace equation. In Fig. 2 we show how the potential becomes nonlinear, paraboliclike, close to the metal gate. For the electron, the potential is confined by a parabolic potential in the radial (ρ) coordinate. Since the Laplacian is zero, the potential in the z direction must compensate for this and is therefore an upside-down parabolic potential. The electron would ''roll down'' toward the substrate, but is effectively stopped because of the barrier material (at $z=-L$). The hole is driven outwards in the radial direction and up to the metal gate (without current flow into the metal). The hole will however be attracted to the electron so there would be an equilibrium for the exciton structure.

III. THEORY

In this section we first give the theory of the exciton lifetime. In Sec. III B we give the theory for the charge density when small external fields are applied. Section III C discusses the Coulomb interaction, including finite boundary conditions in the Hartree equations and the split gate potential in the split gate arrangement.

A. Lifetime of the exciton

The Hamiltonian for the system assumes that an electron and a hole have been created from the vacuum state by laser light. The exciton is created locally, within a volume of atomic size. The energy corresponding to breaking a covalent bond in the ZnO is equal to its band gap $E_G=3.37$ eV at room temperature. Very rapidly after this event the electron and hole wave functions will redistribute (diffuse) and lower the energy by the binding energy of E_0 due to the Coulomb attraction. The observed absorption peak in experimental measurements would then correspond to the transition energy E as

$$E=E_G-E_0. \tag{1}$$

For ZnO the bulk binding energy $E_0=60$ meV and the energy gap $E_G=3.37$ eV at room temperature. We effectively treat the problem as time independent. This is of course a crude approximation since it is known that the excitons have a very short lifetime, typical in the subnanosecond regime. The exciton is then treated as a metastable object. The short lifetime of the exciton will as well affect the polarization of the crystal and this is reflected in that the dielectric constant ε is taken to be an average, chosen here such that the theoretical hydrogenlike ground-state energy will give the correct experimental value. The ground-state energy is ideally given by

$$E_0=-13.6\,\frac{\mu}{\varepsilon^2}\ (eV), \tag{2}$$

where μ is the (dimensionless) effective mass and ε is given in units of the vacuum dielectric constant.

The exact physical mechanism for the annihilation process is very complicated and involves real second quantization physics, and will not be considered here. This process and the strong polar effect of the ZnO material as well as the exciton-phonon interaction will also adjust the effective Coulomb interaction between the electron and the hole. The experimentally fitted value of ε is therefore taking into account phenomena of this kind as well. It is however clear that the annihilation takes place locally (just as it was created locally).

If we calculate the transition rate from the Fermi Golden rule (using the second quantization approach, involving the vacuum state and so on) we obtain the following expression for the lifetime:

$$\frac{1}{\tau}\propto\left|\int \Phi_1(\vec{r})\Phi_2(\vec{r})d^3r\right|^2. \tag{3}$$

Note that this expression is developed using the first-order perturbation theory, this is why it is only approximate. We observe from Eq. (3) that the lifetime could be increased if the hole and the electron wave functions are separated (polarized) by some external potential.

B. Charge density in linear polarization

For the completeness we here briefly describe the theory for weak perturbations of an exciton. The ground state for the hydrogenlike wave function is

$$\Phi\propto e^{i\vec{K}\cdot\vec{R}}e^{-r/a_0}, \tag{4}$$

where $\vec{K}=0$ in the ground state, $\vec{R}=(m_1\vec{r}_1+m_2\vec{r}_2)/(m_1+m_2)$ is the center of mass, m_1 and m_2 are the masses of the electron and the hole, respectively, and $\vec{r}=\vec{r}_1-\vec{r}_2$ is the relative coordinate. However this wave function gives no information of the charges which are involved, and cannot be used to determine the total charge density ϱ (ϱ could be used to calculate different multipole expansions, for example). It is not possible to integrate one of the coordinates using Eq. (4), since the resulting charge density would be totally smeared out over the whole space. This is in fact a

consequence of the Heisenberg uncertainty principle applied for the center of mass, since we in the ground state have specified the momentum $\vec{K}=0$ with exact precision (and hence $\Delta R=\infty$). To obtain a useful definition of a real charge density, we must therefor fix the center-of-mass coordinate (leading to $\Delta K=\infty$). The charge density for particle 1 would then be defined as

$$|\varphi_1(\vec{r}_1)|^2=\int \delta(\vec{R})|\varphi(\vec{r})|^2 d^3r_2, \tag{5}$$

where $\varphi(\vec{r})$ is any wave function in the relative coordinate. Using the definitions of $\vec{R}$ and $\vec{r}$ we would obtain

$$|\varphi_1(\vec{r})|^2=|\varphi(+a_1\vec{r})|^2, \tag{6}$$

$$|\varphi_2(\vec{r})|^2=|\varphi(-a_2\vec{r})|^2, \tag{7}$$

where $a_1=M/m_2$, $a_2=M/m_1$, and $M=m_1+m_2$ (the total mass). If we consider particle 1 to be the proton, the effective Bohr radius (for particle 1) would be $a_0/a_1=a_0m_2/M=a_0/1837$, which corresponds to 24 nuclear radii if we take the proton radius to be 0.2×10^{-15} m. Particle 2 would be the electron and its effective Bohr radius would be $a_0/a_2=a_0m_1/M\cong a_0$, since $m_1\gg m_2$. We define the total charge density ϱ to be

$$\varrho(\vec{r})=N_1|\varphi(a_1\vec{r})|^2-N_2|\varphi(-a_2\vec{r})|^2, \tag{8}$$

where N_1 and N_2 are normalization constants (we define particle 1 to have a positive charge and particle 2 to have a negative charge). As an example we next study an exciton in an external linear electric field E, with equal masses for the electron and the hole (or it could be a positron). The additional perturbation (the electric field is assumed to be small, otherwise the exciton would be unstable and ionize) would be $H'=eE(z_1-z_2)=eEz=eEr\cos\Theta$. Performing a restricted diagonalization of the total Hamiltonian, using only the $1s$ and the $2p$ orbital, we would take the wave function to be

$$\varphi(\vec{r})=c_1\varphi_{1s}(\vec{r})+c_2\varphi_{2p}(\vec{r}), \tag{9}$$

where c_1 and c_2 are determined from the diagonalization eigenvalue problem. Using Eq. (8), Eq. (9) together with Eqs. (6) and (7) and using the antisymmetry rule $\varphi_{2p}(-\vec{r})=-\varphi_{2p}(\vec{r})$ and also that $m_1=m_2=m$, this would yield the total charge density

$$\varrho(\vec{r})=e\frac{128V}{\sqrt{9+64V^2}}\varphi_{1s}(2\vec{r})\varphi_{2p}(2\vec{r}), \tag{10}$$

where $V=eEa_0/E_0$ is the dimensionless potential drop over the Bohr radius a_0. The corresponding two energies are (in units of the ground-state energy) given by $E=(5\pm\sqrt{9+64V^2})/8$, which gives $E=-1$ and $E=-1/4$ when $V\to0$. The charge density in Eq. (10) is evidently positive for $z>0$ and negative for $z<0$ (if not $V=0$), just as we intuitively expect it to be. Note also that the size of the charge distribution is scaled with a factor 2 (i.e., it becomes a factor 2 times smaller than the original wave functions). Of course, this approximation is only valid for $V\ll1$ as we have only expanded the wave function in two orbitals. It is also clear from this analysis that the overlap will increase as V increases [i.e., between φ_1 and φ_2 in Eqs. (6) and (7)]. Therefore, the lifetime would also increase, as can be seen from Eq. (3).

C. Hartree theory for excitons with a boundary-condition dependent Hamiltonian

We will now study strongly nonlinear polarization of the exciton by using a real split gate arrangement, shown in Fig. 1. In addition we will also study excited states and the oscillation strength for the internal optical transitions. In this theory we ignore the Bloch functions and details from band theory, such as nonparabolic dispersion relations and splitting of the valence band (light and heavy holes).

The Hamiltonian (in scaled units) for the electron and the hole within the split gate arrangement (which creates the nonlinear potential) is generally given by

$$\hat{H}=-\frac{\mu}{m_1}\nabla_1^2-\frac{\mu}{m_2}\nabla_2^2+U(\vec{r}_1,\vec{r}_2)+E_c(\vec{r}_1)+E_v(\vec{r}_2), \tag{11}$$

where m_1 and m_2 are the effective masses for the electron and the hole, respectively. The reduced mass is given by $\mu=m_1m_2/(m_1+m_2)$. The last two terms are heterostructure barriers for the electron (E_c) and the hole (E_v). The Hamiltonian is expressed in dimensionless units using the scaling relation $E'=E_0E$ for the energy and $r'=a_0r$ for the distances. The bulk ground-state energy E_0 and the Bohr radius a_0 are expressed through the relations $E_0=\hbar^2/2\mu a_0^2=(e^2/4\pi\epsilon a_0)/2$ and $a_0=2(\hbar^2/2\mu)/(e^2/4\pi\epsilon)$. For ZnO $a_0=1.89$ nm and $E_0=60$ meV (known from experiment), ϵ is the dielectric constant. The potential part of the Hamiltonian $U(\vec{r}_1,\vec{r}_2)$ takes into account the mutual Coulomb interaction as well as the boundary conditions given on the split gate structure and could be expressed through Greens relation

$$\nabla_1\cdot[\tilde{\epsilon}\cdot\nabla_1U(\vec{r}_1,\vec{r}_2)]=2\times4\pi\delta(\vec{r}_1-\vec{r}_2), \tag{12}$$

where the factor 2 stems from the scaling of the Hamiltonian. The "tilde" on the dielectric constant indicates that it could be a coordinate dependent tensor in general. The dielectric constant ϵ for the bulk ZnO depends on the frequency in general. For stationary electric fields $\epsilon=7.2$ and for high frequencies (optical) $\epsilon=3.7$. Since the lifetime of the exciton is very short (corresponding to high frequency), the problem should in principle be solved using dynamical screening, but for simplicity we treat the problem as a time-independent problem. We therefore take an average of the dielectric constant (in between the two limits of ϵ) to be $\epsilon=6.33$, since this would give the correct ground-state energy $E_0=-60$ meV for a bulk exciton in ZnO.

With no confinement, special boundary conditions, and using a constant isotropic dielectric constant (in scaled units $\epsilon=1$) the solution of Eq. (12) becomes

$$U(\vec{r}_1,\vec{r}_2) = -\frac{2}{|\vec{r}_1-\vec{r}_2|}. \tag{13}$$

With the common Coulomb potential given in Eq. (13), the solution of the Hamiltonian (11) (now in real units) is given by Eq. (2). In the scaled units the ground-state energy $E_0=-1$. The effective mass for the hole in ZnO is anisotropic with the values $m_{p//}=0.45$ and $m_{p\perp}=0.59$. We take an average $m_1=(m_{p//}+2m_{p\perp})/3$. The effective mass for the electron is $m_e=0.275$ and is isotropic. This yields the reduced mass $\mu=0.177$.

We now include confinement and boundary conditions in the potential $U(\vec{r}_1,\vec{r}_2)$. On the top of the ZnO surface (see Fig. 1) the metal gate would provide a constant potential V_G (gate potential) relative to the grounded substrate. We would hence have Dirichlet boundary conditions on these surfaces. Depending on the sign of the charge, the electron and the hole will be driven towards the metal gate or the substrate. If V_G alters sign, the electric field will also be turned upside down (see Fig. 2).

The potential term $U(\vec{r}_1,\vec{r}_2)$ will now be treated as follows. When we include the boundary conditions we could formally write the solution as[21]

$$U(\vec{r}_1,\vec{r}_2) = -\frac{2}{|\vec{r}_1-\vec{r}_2|} + F_1(\vec{r}_1)|_{\vec{r}_2} + F_2(\vec{r}_2)|_{\vec{r}_1}. \tag{14}$$

This equation evidently satisfies

$$\nabla^2 U(\vec{r}_1,\vec{r}_2) = 8\pi\delta(\vec{r}_1-\vec{r}_2), \tag{15}$$

if F_1 and F_2 are homogeneous solutions to Eq. (15). The subscripts on F_1 and F_2 indicate that these variables are partially kept constant, so that, for example, F_1 is a function only of the $\vec{r}_1$ coordinate. This would actually be the case when we try to solve Newton's time-dependent equations (i.e., we derive the force on particle 1 from F_1 and the Coulomb term, and must hold the coordinate of particle 2 fixed). For further simplification we define two potentials $U_1(\vec{r}_1,\vec{r}_2) = -2/|\vec{r}_1-\vec{r}_2| + F_1(\vec{r}_1)|_{\vec{r}_2}$ and $U_2(\vec{r}_1,\vec{r}_2) = -2/|\vec{r}_1-\vec{r}_2| + F_2(\vec{r}_2)|_{\vec{r}_1}$. We now impose the boundary conditions on either U_1 or U_2 separately. With the Hamiltonian written in this form, we could easily derive the effective Hartree equation with the total wave function $\Psi(\vec{r}_1,\vec{r}_2)=\Phi_1(\vec{r}_1)\Phi_2(\vec{r}_2)$, which gives

$$-\frac{\mu}{m_1}\nabla^2\Phi_1 + \left[\int U_1(\vec{r}_1,\vec{r}_2)|\Phi_2(\vec{r}_2)|^2 d^3r_2\right]\Phi_1 + E_c\Phi_1 = \lambda_1\Phi_1, \tag{16}$$

$$-\frac{\mu}{m_2}\nabla^2\Phi_2 + \left[\int U_2(\vec{r}_1,\vec{r}_2)|\Phi_1(\vec{r}_1)|^2 d^3r_1\right]\Phi_2 + E_v\Phi_2 = \lambda_2\Phi_2. \tag{17}$$

The effective potentials in Eqs. (16) and (17) should hence incorporate the true boundary conditions. This would be difficult to ensure, using straightforward integration, since we do not know explicitly the expressions for F_1 and F_2 (which also include the boundary conditions). We could hence derive the Poisson equation for the effective potentials in the integrals, denoted by V_1 and V_2. We give the derivation for V_1 here as

$$\nabla_1^2 V_1(\vec{r}) = \nabla_1^2\int U_1(\vec{r}_1,\vec{r}_2)|\Phi_2(\vec{r}_2)|^2 d^3r_2 = 8\pi\int \delta(\vec{r}_1-\vec{r}_2)|\Phi_2(\vec{r}_2)|^2 d^3r_2 = 8\pi|\Phi_2(\vec{r})|^2, \tag{18}$$

where we have used Eq. (15). The equation for V_2 is similar. Finally the boundary condition is taken on V_1 (or V_2) as a whole. In this way we have got around the difficult problem of first solving the exact (boundary-condition dependent) Hamiltonian and we do not need to care about explicitly the information in F_1 and F_2. Using this picture, the boundary condition for the hole (V_1) is set to V_G at the gate and for the electron we shall set $-V_G$ at the gate (since it has opposite charge). It is instructive to study two limits of this potential formalism. First we note that we work with energy potentials (and not electric potentials). In the ''limit'' when we turn off the Coulomb interaction (i.e., when $|\Phi_2(\vec{r})|^2\to 0$) we would obtain the two separate potentials. For a negative gate potential $-V_G$, the electric field would be oriented from the substrate to the metal gate. The hole would then be driven towards the metal gate. The electron (with opposite charge) would hence be driven towards the substrate with the same applied gate voltage (that is why we apply the boundary condition at the gate with opposite sign for the electron). In the other limit, when we turn off the gate voltage and extend the gate boundary to infinity, the resulting potential would simply be the pure Coulomb interaction. Note that this theory does not take into account, for image charges, this is why its result will be only approximate. However, the theory is good enough to give the right trends. The physical consequence of the image charges is that the positive charge (hole), located close to the metal gate will be screened by the image charge. Therefore, the Coulomb interaction will be reduced, leading to another balance between the gate voltage and the Coulomb interaction. Effectively, this screening can then be compensated with a larger value of the gate voltage, and would hence not affect the major trend of the polarization phenomenon.

We use cylindrical symmetry for obtaining a ground state and a few excited states. The total wave function is given by

$$\Psi(\vec{r}_1,\vec{r}_2) = \varphi_1(\rho_1,z_1)e^{iM_1\alpha_1}\varphi_2(\rho_2,z_2)e^{iM_2\alpha_2}, \tag{19}$$

where M_1 and M_2 are (integer) quantum numbers for the electron and hole, respectively. Thus, for example, $|\Phi_1(\vec{r}_1)|^2=|\varphi_1(\rho_1,z_1)|^2$. For the case that we want to study, the excited states, the quantum numbers M_1 and M_2 should be included in the Schrödinger equations as

$$-\frac{\mu}{m_1}\left[\frac{\partial}{\partial\rho}\left(\rho\frac{\partial\varphi_1}{\partial\rho}\right)+\rho\frac{\partial^2\varphi_1}{\partial z^2}\right]+\left[\rho(V_1+E_c(z))+\frac{\mu M_1^2}{m_1\rho}\right]\varphi_1 = \lambda_1\rho\varphi_1, \tag{20}$$

$$-\frac{\mu}{m_2}\left[\frac{\partial}{\partial\rho}\left(\rho\frac{\partial\varphi_2}{\partial\rho}\right)+\rho\frac{\partial^2\varphi_2}{\partial z^2}\right]+\left[\rho(V_2+E_v(z))+\frac{\mu M_2^2}{m_2\rho}\right]\varphi_2 = \lambda_2\rho\varphi_2, \tag{21}$$

where V_1 is defined from Eq. (18) (also in cylindrical coordinates), and similarly for V_2. The total dimensionless energy E_0 (binding energy) for the exciton must be calculated as follows. If we just add λ_1 and λ_2, we would have double counted the Coulomb term $2/r_{12}$, so we must therefore subtract one of them. Hence the total energy would be given by

$$E_0=\lambda_1+\lambda_2+2\int|\Phi_1(\vec{r}_1)|^2\left[\int\frac{|\Phi_2(\vec{r}_2)|^2}{|\vec{r}_1-\vec{r}_2|}d^3r_2\right]d^3r_1. \tag{22}$$

We calculate the Coulomb integral by solving Poisson's equation [in principle the same equation as Eq. (18)] and then integrating the well behaved potential. For this case we transfer the solutions from the Schrödinger equations to a new geometry, without the split gate boundary (a huge geometry relative to the typical size of the exciton structure).

D. Optical transitions in the exciton

Here we consider optical transitions from the ground state to some excited states, particularly the one with the largest oscillator strength. We use the dipole transition approximation here. The optical (two-body) perturbation of the Hamiltonian is considered as the light comes in to the ZnO surface in the z direction. The electromagnetic field components are then oriented in the x-y plane. The perturbation H' is then taken to be

$$H'=\frac{eA_x}{2m_1}\hat{p}_{1x}-\frac{eA_x}{2m_2}\hat{p}_{2x}, \tag{23}$$

where A_x is the magnetic vector potential in the x direction. From this perturbation we obtain the oscillator strength f_{ij} between the state i to the state j as

$$f_{ij}=\frac{2\mu\omega_{ij}}{\hbar}|\langle i|x_1-x_2|j\rangle|^2=E'_{ij}|\langle i|x'_1-x'_2|j\rangle|^2, \tag{24}$$

where $E_{ij}=E_i-E_j$, $\omega_{ij}=E_{ij}/\hbar$, $E'=E_0E$, $E_0=\hbar^2/2\mu a_0^2$, and $x'=a_0x$, where a_0 is the Bohr radius. Note that f_{ij} is dimensionless. Here the primes indicate only that the corresponding properties are dimensionless. The wave functions are given from Eq. (19). Simplifying this a bit further leads us to the final result (now omitting the primes for a simpler notation):

$$f_{ij}=\frac{E_{ij}}{4}[\,\delta_{|M_{1i}-M_{1j}|,1}\delta_{M_{2i},M_{2j}}\langle\varphi_{1i}|\rho|\varphi_{1j}\rangle\langle\varphi_{2i}|\varphi_{2j}\rangle - \delta_{|M_{2i}-M_{2j}|,1}\delta_{M_{1i},M_{1j}}\langle\varphi_{2i}|\rho|\varphi_{2j}\rangle\langle\varphi_{1i}|\varphi_{1j}\rangle]^2, \tag{25}$$

where it is understood that the volume element in all the integrations in Eq. (25) should be taken as $2\pi\rho d\rho dz$ (the angular integration over α has already resulted in the factor 1/4 when $\Delta M=\pm1$). We can see from Eq. (25) what the transition rules are. If, for example, the holes have an excited state with $M_{2j}=1$ (and in the ground state $M_{2i}=0$), then we must set $M_{1i}=M_{1j}$ ($=0$ for the ground state). Indeed, one of the two terms in Eq. (25) will always be zero. The overlap integral $\langle\varphi_{1i}|\varphi_{1j}\rangle$ for the hole is roughly equal to 1 for small values of the gate voltage (and also for large values). In the intermediate case, the overlap could be very small in some cases.

IV. RESULTS

A. Parameters and boundary conditions for the system

The radius of the circular gate hole on the ZnO layer (see Fig. 1) has a value of $5a_0=9.45$ nm in all calculations. The distance from the metal gate to the grounded substrate was $80a_0=151$ nm (corresponding to 291 atomic layers of ZnO). The total radius for the whole geometry was set to $120a_0$ and we also included the volume above the split gate with a distance $80a_0$ (to get rid of image charge effects at the circular opening in the metal gate at the ZnO surface). Then the split gate metal represents a cut in our geometry with a constant potential V_G (or $-V_G$, depending on which charge we solve the Poisson equation for) set as the boundary condition. The mesh is set to be very fine in the regions $0<\rho<5$ and $-5<z<0$, and a fine mesh in the regions $5<\rho<20$ and $-5<z<0$. The rest of the structure has a rough mesh (we use totally ~3000 grid points).

At $\rho=120$ we apply Neumann boundary conditions for the Poisson equation, since this results in a linear potential drop from the metal gate to the substrate for large radii. At $\rho=0$, we also apply Neumann boundary conditions for both Poisson's and Schrödinger's equations. Strictly speaking this is not a physical boundary condition and must be introduced artificially because of the cylindrical coordinate weight function ρ. At $z=-80$ we have the substrate, where we apply Dirichlet boundary conditions. We also set the potential to be zero at $z=+80$.

For the Schödinger equations we apply hard walls everywhere, except for $\rho=0$ (described previously). Just above the metal we set the potential barrier to 3 eV for the boundary purpose (which could correspond to an oxide layer or vacuum). The metal thickness was set to $5a_0$. In general, we therefore expect the electron (or the hole) to penetrate through this barrier a little bit (i.e., for $z>0$).

B. Numerical results

The self-consistent Hartree calculations of the exciton in the split gate arrangement have been performed for three

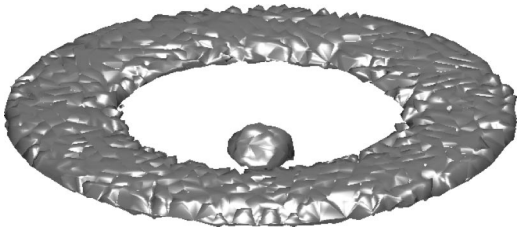

FIG. 3. The ring exciton shown for $V_G=-4.8$ V. The ring is thin and is located close to the metal gate surface. The electron ''dot'' is located close to the barrier material.

different cases. The first case is when the ZnO layer has a thickness of $5a_0=9.45$ nm and the potential barrier is set to 1 eV for both the electron and the hole. The second case is when the barrier is reduced to 0.2 eV and the ZnO thickness is $5a_0$. Finally the third case is when the ZnO thickness is reduced to $4.5a_0$ and the barrier is 1 eV. All properties such as the ground-state energy E_0, the lifetime τ, the overlap, the excitation energies E_{ij}, and the oscillator strength f_{ij} are investigated as functions of the split gate voltage V_G, which runs in the range 0 V to -4.8 V (-4.8 V corresponds to the dimensionless value $eV_G/E_0=-80$). In this section we have chosen to present the figures using the absolute value of V_G on the positive x axis, which is indicated with (negative) in the figure captions. A use of both positive and negative values of V_G would have given (almost) symmetric curves around $V_G=0$. In addition, we also study how the ground-state energy E_0 and the lifetime τ depend on the ZnO layer thickness L, for the fixed gate voltage $eV_G/E_0=-80$ ($|E_0|=60$ meV).

The probability density for the electron and the hole is shown in a 3D view in Fig. 3 for $V_G=-4.8$ V when $L=5a_0$ and the heterostructure barrier $U_b=1$ eV. The hole forms a ring around the electron, which is displaced downwards relative to the ring (the image is tilted, this is why the electron seems to be displaced from the center). With opposite polarity of the gate voltage the electron would form a ring around the hole.

In Fig. 4 the total charge density is shown in more detail than in the previous figure, for $eV_G/E_0=-80$, -40, and 0. The axes are given in units of the Bohr radius a_0. Note that the overlap between the hole and the electron wave functions is very small for $eV_G/E_0=-80$ and -40. With no applied voltage, the exciton is close to a bulk exciton. Because of the different effective masses, the charge density ϱ [compare with Eq. (8)] is not zero. The probability densities for the electron and the hole are slightly more broader than the contours in this figure [compare with the factor 2 in Eq. (8)]. Since the hole is very close to the metal surface, a polarization in the metal could adjust the potential for the hole (i.e., this effect is commonly referred to as the effect of image charges). However, the effect of image charges is not included in the present paper. Because of the closeness of the metal gate to the hole, the Coulomb interaction will be screened appreciably, leading to a reduction of the exciton binding energy.

In Fig. 5 the binding energy E_0 is plotted for the exciton in the ZnO layer. We compare in this figure three different

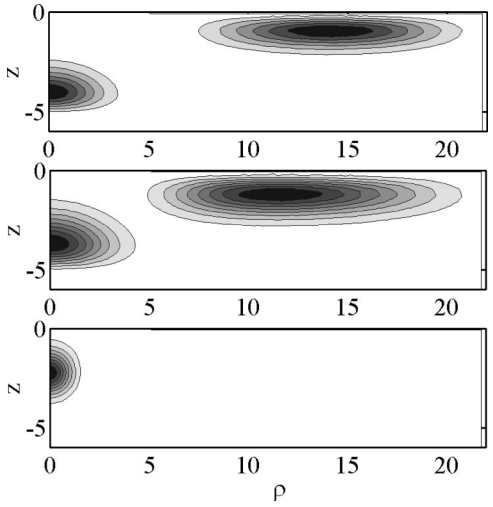

FIG. 4. The charge density for the exciton shown in the (scaled) cylindrical coordinates, for $eV_G/E_0=-80$, -40, and 0, from top to bottom. $L=5a_0$ (ZnO thickness) for this figure.

cases when the ZnO thickness and the barrier height are varied. As can be seen, a decrease of the barrier potential would also decrease the energy. As the ZnO thickness is decreased the energy will increase (this is a typical quantum well phenomena). The energy changes drastically at $V_G=-2$ V (the figure shows the absolute value of V_G). This threshold voltage is directly connected with the structural transition of the exciton, shown in Fig. 4. The reason for this threshold voltage is that the nonlinear potential drop of the split gate potential has to be increased (in magnitude) until it becomes of the same order as the bulk ground-state energy (60 meV). When this critical potential drop has been reached, the bulk-like exciton configuration would not be stable any more. This effect is indeed a type of a structural transition, which also has been reported by Janssens *et al.*[14] in a two-dimensional type II quantum dot.

The typical potential drop that is required (or in other words, the threshold voltage which is required) would depend on the metal gate radius and the total distance between

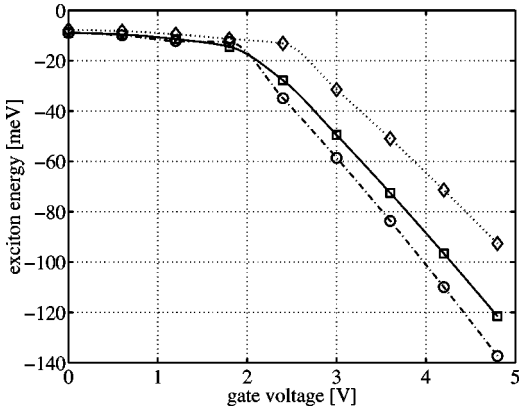

FIG. 5. Binding energy E_0 in ZnO (quantum well like) as a function of the gate voltage V_G (negative). $L=5a_0$ and $U_b=1$ eV (squares), $L=5a_0$ and $U_b=0.2$ eV (circles), and $L=4.5a_0$ and $U_b=1$ eV (diamonds).

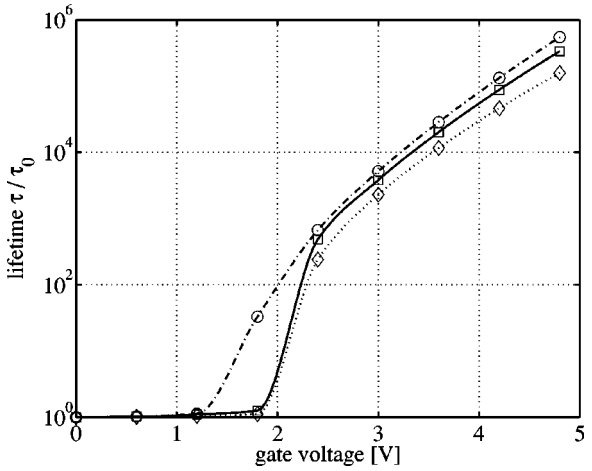

FIG. 6. Lifetime τ as a function of the gate voltage V_G (negative) for the exciton ground state. $L=5a_0$ and $U_b=1$ eV (squares), $L=5a_0$ and $U_b=0.2$ eV (circles), and $L=4.5a_0$ and $U_b=1$ eV (diamonds).

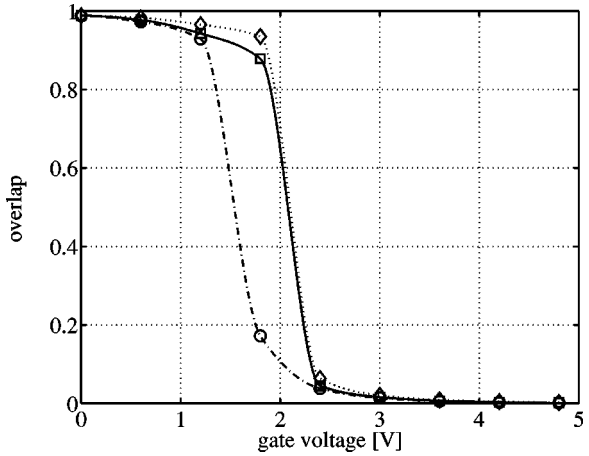

FIG. 7. Overlap $\langle 1|2\rangle$ between the electron and the hole wave function as a function of the gate voltage V_G (negative) for the exciton ground state. $L=5a_0$ and $U_b=0.2$ eV (circles) and $L=4.5a_0$ and $U_b=1$ eV (diamonds).

the substrate and the metal gate. An analysis of different sizes have not been made but we expect to see exactly the same phenomena and the same E_0-V_G curve. The only difference would be that the threshold voltage would be different and that the slope in the E_0-V_G curve would be different.

A special separate calculation was made for the bulk exciton using the Hartree method (but now with a very large geometry and without any metal gate). The result shows that the Hartree energy is $E_0=-0.411$ which should be compared with exact value $E_0=-1$ (in dimensionless units). This example shows that the Hartree theory does not give accurate results (60% error) when the electron and the hole are extremely correlated. However, the strong correlation (defined as the difference between the exact energy and the Hartree energy) takes place only when the overlap between the electron and the hole wave functions are large (around 1), i.e., this means that we can trust the Hartree calculation first when it is shown that the overlap is small. For the exciton in the ground state this is the case when $V_G<-2$ V. A possible way of solving this strongly correlated problem exactly could be by the use of the path integral Monte Carlo technique (see, for example, Ref. 22 and the references therein). It is also interesting to note that type II quantum dots separate the electron and the hole, such that the overlap (normally) becomes small. For this case a Hartree calculation would give a satisfactory result (see, for example, Janssens *et al.*[14]).

There is limit to how much the exciton can be polarized. It should not take longer time for the hole or the electron to move to their self-consistent positions than the typical lifetime of the bulk exciton. An estimation, using Ehrenfest theorem gives the time $t\approx\sqrt{2m_2/E_0}\Delta\rho$ for the hole to move from the ''creation center'' of the exciton to its equilibrium position (see Fig. 4). Using $\Delta\rho=14$, $E_0=60$ meV, and $m_2=0.5m_e$ gives a time of 0.25 ps, which is much shorter than a typical exciton lifetime of 1 ns.

In Fig. 6 the lifetime τ [see Eq. (3)] is plotted as a function of the gate voltage (in units of the bulk lifetime). In this figure it is also clear that there is a dramatic change at a typical threshold voltage of $V_G=-2$ V. The bulk exciton lifetime is typical of the order 1 ns for ZnO. The transition is less sharper for the low barrier $U_b=0.2$ eV than for the other cases with a large barrier $U_b=1$ eV. The long lifetime is a consequence of the small overlap between the electron and the hole wave functions. Evidently, the dramatic change in the lifetime gives a fingerprint of the fact that a structural transition has occurred (which is evident from Fig. 4).

In Fig. 7 the overlap integral is plotted as a function of the gate voltage. The overlap is roughly inversely proportional to the lifetime. For $V_G<-2.2$ V the overlap is very small, and we therefore expect the Hartree calculation to be very accurate in this region, since the correlation between the electron and the hole wave function is very small here. For $U_b=0.2$ eV (the dash-dotted line) we could observe an intermediate point at $V_G=-1.8$ V and $\langle 1|2\rangle=0.19$. A charge density plot shows that this corresponds to the case when the hole is starting to diffuse into the central region of the gate structure ($\rho=0$), meanwhile it still has a ringlike shape.

The penetration of the electron wave function into the barrier is shown in Fig. 8 at $\rho=0$. It is clear from the figure that the barrier potential is decreasing for large values of $|z|$, due to the electric field between the metal gate and the substrate. Hence, this figure shows that the exciton is a metastable object when it is polarized by a split gate potential. For excited states the effective tunneling barrier becomes even lower. To avoid tunneling of the electron to the substrate we must introduce an artificial hard wall at $z=-13$ for the ground state and at $z=-9$ for excited states. From the WKB theory we could estimate the tunneling time $\propto\hbar/E_0|t|^2$, where $|t|^2$ is the usual tunneling probability. For the ground state this time is in practice infinite, but for the excited states the time could be much smaller.

The metastability of the exciton could however be interesting for a possible practical use. For excited states using low barriers, the electron could in principle tunnel through the barrier if these levels are populated by a THz radiation. Such ''splitting'' of the exciton would result in an electrical

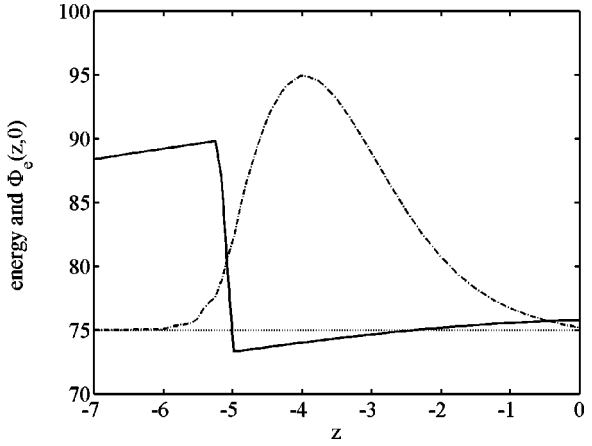

FIG. 8. Tunneling of the electronic wave function into the barrier for $V_G=-4.8$ V for $\rho=0$. $L=5a_0$ and $U_b=1$ eV.

signal which could be detected. This will of course only happen if the lifetime of the exciton is sufficiently long so that an excited state could be populated. Alternatively the excited state could serve as the second level in a qubit (the situation is similar to the metastable states in Josephson-junction washboard potential).

In Figs. 9 and 10 the ground-state energy and the lifetime ($\tau_0=1$ ns) are plotted as a function of the ZnO thickness L, when the gate voltage is $V_G=-4.8$ V. For this voltage we have the typical ring structure and Fig. 9 shows that the energy changes linearly with the ZnO thickness. In a thick ZnO layer it is possible for the electron to be located at a large distance from the hole than it would be for a thin layer. The lifetime changes exponentially with the layer thickness (this is also a consequence of a large separation between the electron and the hole).

In Figs. 11 and 12 the optical transition from the ground state to an excited state with a dominating oscillator strength is shown. Figure 11 shows the transition energy converted to frequency (in THz) and Fig. 12 shows how the corresponding oscillator strength is changing with the gate voltage. We classify the excited states with the set of quantum numbers N_1, M_1, N_2, and M_2. N_1 and N_2 give the principal quantum numbers for the electron and the hole, respectively, when the quantum number M is fixed. $N_1=1$ and $M_1=0$ is the ground state for the electron and so on. The quantum numbers M_1 and M_2 give rise to centrifugal potentials for the electron and the hole. The selected (allowed) excited state in Figs. 11 and 12 correspond to $N_1=1$ and $M_1=1$ for the electron, meanwhile the hole is in its ''old ground state'' $N_2=1$ and $M_1=0$. The Schrödinger and Poisson equations were solved self-consistently to obtain these excited states.

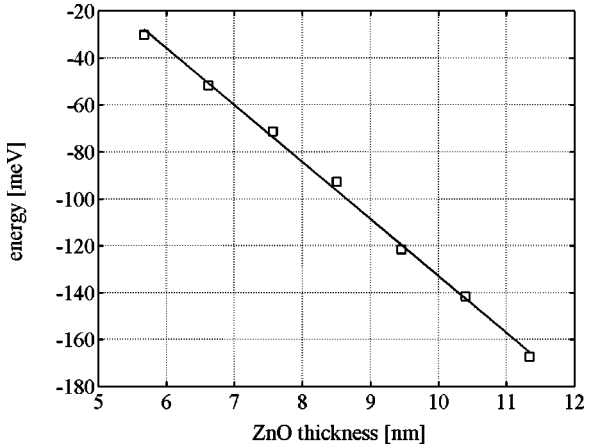

FIG. 9. Binding energy E_0 as a function of the thickness of the ZnO layer for $V_G=-4.8$ V and $U_b=1$ eV.

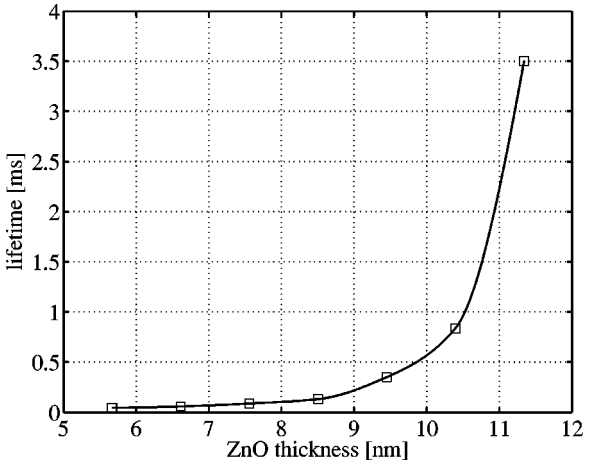

FIG. 10. Lifetime τ as a function of the thickness of the ZnO layer for $V_G=-4.8$ V and $U_b=1$ eV.

As a comparison we give the values of the first four allowed excited states, labeled (i), (ii), (iii), and (iv), for the gate voltage $V_G=-4.8$ V: (i) For $N_1=1$, $M_1=1$, $N_2=1$, and $M_2=0$, $\Delta E=12.31$ meV and $f_{ij}=0.322$; (ii) For $N_1=2$, $M_1=1$, $N_2=1$, and $M_2=0$, $\Delta E=27.71$ meV and $f_{ij}=0.002$; (iii) For $N_1=1$, $M_1=0$, $N_2=1$, and $M_2=1$, $\Delta E=0.04$ meV and $f_{ij}=0.032$; and (iv) For $N_1=1$, $M_1=0$, $N_2=2$, and $M_2=1$, $\Delta E=2.87$ meV and $f_{ij}=0.099$.

The first transition is dominating, first as the oscillator strength is large for this transition and second as it corre-

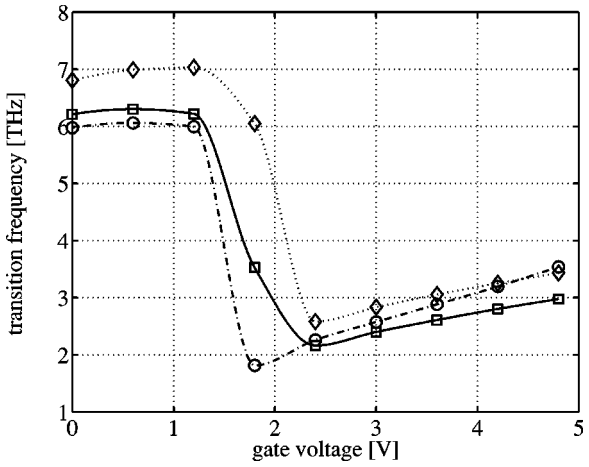

FIG. 11. The optical transition frequency from the ground state for the dominating peak, as a function of the gate voltage V_G (negative). $L=5a_0$ and $U_b=0.2$ eV (circles) and $L=4.5a_0$ and $U_b=1$ eV (diamonds).

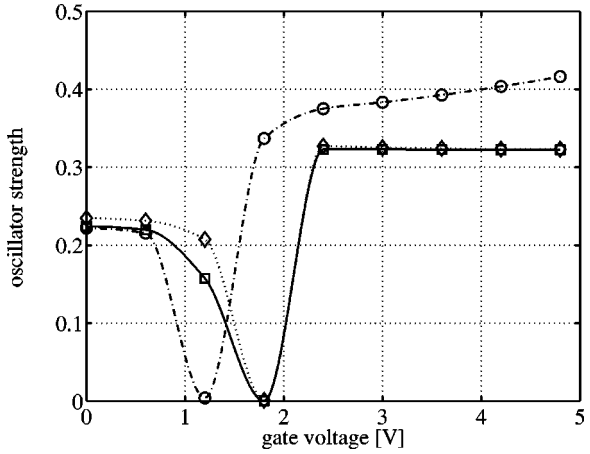

FIG. 12. The oscillator strength for the optical transition between the ground state and the excited state $M_1=1$, as a function of the gate voltage V_G (negative). $L=5a_0$ and $U_b=0.2$ eV (circles) and $L=4.5a_0$ and $U_b=1$ eV (diamonds).

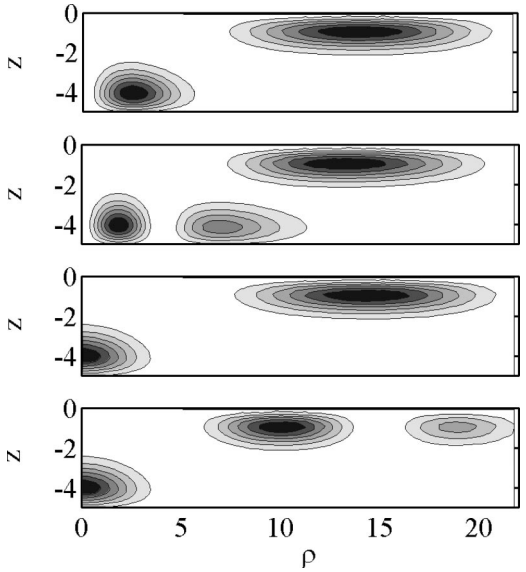

FIG. 13. Different self-consistent excited states for the exciton in the ρ-z plane. The first figure from top to bottom is classified by the quantum numbers $N_1=1$, $M_1=1$, $N_2=1$, and $M_2=0$. The second figure has the quantum numbers $N_1=2$, $M_1=1$, $N_2=1$, and $M_2=0$. The third figure has the quantum numbers $N_1=1$, $M_1=0$, $N_2=1$, and $M_2=1$. Finally the fourth figure has the quantum numbers $N_1=1$, $M_1=0$, $N_2=2$, and $M_2=1$. $eV_G/E_0=80$, $L=5a_0$, and $U_b=1$ eV.

sponds to an energy which is possible to detect in an optical experiment (too small energies could not be seen in optical measurements). The second transition has a large transition energy but has a small oscillator strength. The third transition has both a small transition energy and oscillator strength. Finally, the fourth transition has an oscillator strength comparable with the first dominating transition, but has much lower energy.

The different self-consistent (allowed) excited states are finally shown in Fig. 13. The previously mentioned transition cases (i), (ii), (iii), and (iv) are shown from top to bottom in the figure. The top figure shows the dominating excited state (i.e., the transition from the ground state to this excited state is dominating since the oscillator strength is large). In the second figure (ii), the electronic wave function has two different modes with opposite signs of the wave function (located at $\rho=2$ and $\rho=7$). The oscillator strength for this case would therefore be very low.

V. CONCLUSIONS

In this paper we show that an exciton in a thin ZnO layer could be strongly polarized using a split gate potential. Due to the large separation between the electron and the hole we also show that the lifetime for the exciton will increase from the nanosecond regime to the millisecond regime. The structural transition of the exciton takes place at a certain threshold voltage. The exciton ground-state energy was calculated using a self-consistent Schrödinger-Poisson technique and the results show that the energy could be varied to 120 meV for an applied negative gate voltage of -5 V. Since the lifetime is long for the polarized ''phase'' of the exciton structure, above the threshold voltage, we also calculated the optical transition energy/frequency and the oscillator strength for a self-consistent excited state which would be the most dominating and sharp peak that would appear in experiments. We discuss the metastable nature of the exciton in this kind of heterostructure and conclude that especially excited states may tunnel out from the heterostructure barrier. This effect could be used as a tunable THz detector. We hope that our calculations, made on a realistic structure would stimulate future experimental research.

ACKNOWLEDGMENTS

The work was funded by SSF-Quantum Devices.

*Email address: sunkan@fy.chalmers.se

[1] P.Y. Yu and M. Cardona, *Fundamentals of Semiconductors, Physics and Material Properties* (Springer, New York, 1996).
[2] M.F. Crommie, C.P. Lutz, and D.M. Eigler, Nature (London) **363**, 524 (1993).
[3] G. Bastard, *Physics and Applications of Quantum Wells and Superlattice* (Plenum, New York, 1987).
[4] T. Chakraborty, *Quantum Dots* (Elsevier, Amsterdam, 1999).
[5] V. Halonen, T. Chakraborty, and P. Pietiläinen, Phys. Rev. B **45**, 5980 (1992).
[6] K.L. Janssens, B. Partoens, and F.M. Peeters, Phys. Rev. B **65**, 233301 (2002).
[7] K.L. Janssens, B. Partoens, and F.M. Peeters, Phys. Rev. B **66**, 075314 (2002).
[8] P.O. Holtz, S. Wongmanerod, B. Sernelius, G. Pozina, J.P. Bergman, L.D. Madsen, J.P. McCaffrey, K. Reginski, M. Bugajski, M. Godlewski, J. Thordson, and T.G. Andersson, *Compound Semiconductor Power Transistors and State-of-the-Art Program on Compound Semiconductors (SOTAPOCS XXIX)* (Electrochemical Society, Pennington, USA, 1998).

[9] H. Mathieu, P. Lefebvre, and P. Christol, Phys. Rev. B **46**, 4092 (1992).
[10] L.C. Andreani and A. Pasquarello, Phys. Rev. B **42**, 8928 (1990).
[11] W. Ospina, P. Aristizabal, R.L. Restrepo, A. Montes, and C.A. Duque, Phys. Status Solidi B **220**, 131 (1999).
[12] K. Chang and F.M. Peeters, J. Appl. Phys. **88**, 5246 (2000).
[13] H. Büttner and J. Pollman, Physica B & C **117B&118B**, 278 (1983).
[14] K.L. Janssens, B. Partoens, and F.M. Peeters, Phys. Rev. B **64**, 155324 (2002).
[15] F.V. Kyrychenko, S.M. Ryabchenko, and Yu.G. Semenov, Physica E (Amsterdam) **8**, 275 (2000).
[16] O. Betbeder-Matibet and M. Combescot, Phys. Rev. B **54**, 11 375 (1996).
[17] Yu.E. Lozovik and I.V. Ovchinnikov, Phys. Rev. B **66**, 075124 (2002).
[18] Yu.E. Lozovik, I.V. Ovchinnikov, S.Yu. Volkov, L.V. Butov, and D.S. Chemla, Phys. Rev. B **65**, 235304 (2002).
[19] N.S. Averkiev and A.M. Monakov, Zh. Eksp. Teor. Fiz. **97**, 912 (1990) [Sov. Phys. JETP **70**, 512 (1990)].
[20] E.L. Ivchenko and G.E. Pikus, *Superlattices and Heterostructures—Symmetry and Optical Phenomena* (Springer-Verlag, Heidelberg, 1997).
[21] J.D. Jackson, *Classical Electrodynamics* (Wiley, New York, 1975).
[22] P.A. Sundqvist, Yu. Volkov, Yu.E. Lozovik, and M. Willander, Phys. Rev. B **66**, 075335 (2002).